

RESEARCH

Open Access



Comparative structure and evolution of the organellar genomes of *Padina usoehtunii* (Dictyotales) with the brown algal crown radiation clade

Yi-Jia Liu¹, Tong-Yun Zhang¹, Qi-Qi Wang¹, Stefano G. A. Draisma^{2*} and Zi-Min Hu^{1*}

Abstract

Background Organellar genomes have become increasingly essential for studying genetic diversity, phylogenetics, and evolutionary histories of seaweeds. The order Dictyotales (Dictyotophycidae), a highly diverse lineage within the Phaeophyceae, is long-term characterized by a scarcity of organellar genome datasets compared to orders of the brown algal crown radiation (Fucophycidae).

Results We sequenced the organellar genomes of *Padina usoehtunii*, a representative of the order Dictyotales, to investigate the structural and evolutionary differences by comparing to five other major brown algal orders. Our results confirmed previously reported findings that the rate of structural rearrangements in chloroplast genomes is higher than that in mitochondria, whereas mitochondrial sequences exhibited a higher substitution rate compared to chloroplasts. Such evolutionary patterns contrast with land plants and green algae. The expansion and contraction of the inverted repeat (IR) region in the chloroplast correlated with the changes in the number of boundary genes. Specifically, the size of the IR region influenced the position of the boundary gene *rp121*, with complete *rp121* genes found within the IR region in Dictyotales, Sphacelariales and Ectocarpales, while the *rp121* genes in Desmarestiales, Fucales, and Laminariales span both the IR and short single copy (SSC) regions. The absence of the *rbcR* gene in the Dictyotales may indicate an endosymbiotic transfer from the chloroplast to the nuclear genome. Inversion of the SSC region occurred at least twice in brown algae. Once in a lineage only represented by the Ectocarpales in the present study and once in a lineage only represented by the Fucales. Photosystem genes in the chloroplasts experienced the strongest signature of purifying selection, while ribosomal protein genes in both chloroplasts and mitochondria underwent a potential weak purifying selection.

Conclusions Variations in chloroplast genome structure among different brown algal orders are evolutionarily linked to their phylogenetic positions in the Phaeophyceae tree. Chloroplast genomes harbor more structural rearrangements than the mitochondria, despite mitochondrial genes exhibiting faster mutation rates. The position and the change in the number of boundary genes likely shaped the IR regions in the chloroplast, and the produced structural variability is important mechanistically to create gene diversity in brown algal chloroplast.

*Correspondence:

Stefano G. A. Draisma

stefano.a@psu.ac.th

Zi-Min Hu

huzimin9712@163.com; huzm@ytu.edu.cn

Full list of author information is available at the end of the article



© The Author(s) 2024. **Open Access** This article is licensed under a Creative Commons Attribution-NonCommercial-NoDerivatives 4.0 International License, which permits any non-commercial use, sharing, distribution and reproduction in any medium or format, as long as you give appropriate credit to the original author(s) and the source, provide a link to the Creative Commons licence, and indicate if you modified the licensed material. You do not have permission under this licence to share adapted material derived from this article or parts of it. The images or other third party material in this article are included in the article's Creative Commons licence, unless indicated otherwise in a credit line to the material. If material is not included in the article's Creative Commons licence and your intended use is not permitted by statutory regulation or exceeds the permitted use, you will need to obtain permission directly from the copyright holder. To view a copy of this licence, visit <http://creativecommons.org/licenses/by-nc-nd/4.0/>.

Keywords *Padina usoehtunii*, Dictyotales, Phaeophyceae, Chloroplast genome, Mitochondrial genome, Phylogeny, Structural variation, Sequence variation

Background

Semi-autonomous organelles in plant cells arose from ancient endosymbiotic events and subsequently underwent multiple gene transfers and structural modifications [1–3]. Through this evolutionary process, organellar genomes have retained genes for essential organellar functions. Nowadays, with the increased availability of organellar genomes, it has become technically feasible to investigate genome-scale evolution, adaptation, and phylogenetic diversity across the algae tree of life.

The brown algae or Phaeophyceae classified into twenty orders and over 2,000 species [4], representing an essential component of the littoral and sublittoral ecosystems. They originated approximately 185–180 million years ago (Ma) [5]. Fossil evidence, including *Padina* (145.5–99.6 Ma) [6], *Paleocystophora* and *Julescraneia grandicornis* (13–17 Ma) [7], along with the estimates of concatenated organellar genes [8, 9], suggest that the orders Dictyotales and Sphacelariales evolved earlier (> 100 Ma) than Desmarestiales/Laminariales/Ectocarpales (< 100 Ma) [10]. Silberfeld et al. (2010) reported that the order Dictyotales is a member of the SSDO clade (Sphacelariales, Syringodermatales, Dictyotales, and Onslowiales) or Dictyotophycidae that split from the BACR clade (brown algal crown radiation) or Fucophycidae and diversified into orders during the Jurassic (200–175 Ma) [5]. Ectocarpales, Laminariales sensu lato (including Chordales), Fucales, and Desmarestiales belonging to the BACR clade, diversified into orders during the early Cretaceous period (128 Ma). Taxonomically, the identification and classification of new brown algal species primarily relies on morphological characteristics and DNA sequences. Organellar genes in particular have shown better resolution for intraspecific discrimination in certain taxonomic groups compared to the nuclear internal transcribed spacer (ITS) [11]. They have provided essential insights into the origin, phylogenetic structure and biogeographical patterns of brown algae [5, 11–16]. The application of organellar genomes has also been proved instrumental to uncover genetic relationships among individuals and populations, shedding light on adaptive evolution [17].

Most phaeophycean organellar genomes sequenced to date are from members of the Fucophycidae (BACR clade) and only three species of Dictyotophycidae (SSDO clade), one Ishigeophycidae and no Discosporangiophycidae [18]. Notably, the structural and functional interpretation and comparison of the available organellar

genomes seldom connected to the phylogenetic structure and timing of the brown algal tree of life. For example, Liu et al. (2018) compared mitochondrial and chloroplast genomes of *Sargassum confusum* (Fucales) and examined gene content and sequence conservation [19]. They found distinct evolutionary characteristics between the two organellar genomes in terms of A + T content, intron content, and stop codon usage, and reported that mitochondrial genomes exhibited more nucleotide variability than the chloroplast. In addition, Zhang et al. (2022) compared base substitution rates among seven *Sargassum* species and found higher mutation rates of mitochondrial genes compared to chloroplast genes [20]. Starko et al. (2021) explored organellar genome rearrangements and evolution in nine orders of brown algae [18]. They also found that mitochondrial genes evolved at a faster rate than chloroplast genes, but that structural rearrangements in chloroplast genomes were more prevalent than in mitochondria. Recent studies successively explored the organellar genome content, gene rearrangement and phylogeny of *Dictyopteris divaricata* in the order Dictyotales [21, 22]. However, these studies either focused on a single genus or individual organellar genome, or biased taxa with data-rich organellar genomes. The limited number of organellar genomes from representatives outside the Fucophycidae may also lead to an incomplete or biased evolutionary interpretation of organellar genomes in the Phaeophyceae.

To comprehensively elucidate the evolution and origin of brown algae, it is imperative to augment the organellar genome database from diverse brown algal taxa. The order Dictyotales represents a diverse and evolutionarily important lineage in the Phaeophyceae [23]. Dictyotalean species are widely distributed in subtropical and tropical oceans and constitute one of the few brown algal taxa with high diversity in the tropics due to the tolerance to a warm climate [24]. Among its diverse genera, the noteworthy genus *Padina* Adanson encompasses 58 currently accepted and formally described species [25], but 63 operational taxonomic units (OTUs) [23]. *Padina usoehtunii* Ni–Ni–Win & H.Kawai is only known from the west coast of the Southeast Asian peninsula, from the Bay of Bengal (Myanmar) to the Malacca Strait (Thailand) where it grows in the intertidal [26–28]. This species can potentially serve as a model for studying lineage diversity and genome evolution of brown algae.

In this study, we sequenced the mitochondrial and chloroplast genomes of *P. usoehtunii*, thereby adding

to the organellar genome dataset of the order Dictyotales, which had previously consisted of two species (*Dictyopteris divaricata* (Okamura) Okamura and *Dictyota dichotoma* (Kuntze) O.Schmidt) within the family Dictyotaceae. Our study focused on the Dictyotales and compared it with five representative brown algal orders, i.e., Sphacelariales (Dictyotophycidae) and Desmarestiales, Laminariales, Ectocarpales, and Fucales (Fucophycidae). Our investigation is centered on the following key aspects among brown algal organelles: 1) organellar genome features; 2) extent of structural rearrangements (inverted repeat regions and gene arrangements); 3) sequence evolutionary differences (nucleotide substitution rates, codon usage bias, and repeat sequences).

Results

Organellar genomes characteristics of *Padina usoehyunii*

The single-circular chloroplast genome of *P. usoehyunii* is 125,291 bp in length (Fig. S1), larger than species of Fucales (124,068–125,066 bp), but smaller than any other previously sequenced brown alga (126,099–139,954 bp) (Table 1). The largest phaeophyceean chloroplast genome (139,954 bp) is found in *Ectocarpus siliculosus* (Dillwyn) Lyngbye (Ectocarpales). The chloroplast genome of *P. usoehyunii* comprises a 72,226 bp Long Single Copy region (LSC), a 41,273 bp Short Single Copy region (SSC), and two 5,896 bp inverted repeats regions (IRa and IRb) (Fig. S1). It contains 173 genes accounting for 78.02% of the chloroplast genome, including 139 protein coding genes (PCGs), 28 transfer RNA (tRNA) genes, and 6 ribosomal RNA (rRNA) genes (Table S1). The *rbcR* and *rpl32* genes were absent in both dictyotaleans, *P. usoehyunii* and *Dictyopteris divaricata*, but present in all six other investigated orders. The *thiS* gene was absent in the Dictyotales, Desmarestiales, and Ectocarpales, and three species of Laminariales (i.e., *Chorda asiatica*, *Laminaria ephemera*, and *Saccharina japonica*), but present in Fucales, Sphacelariales, and two species of Laminariales (i.e., *Alaria marginata* and *Macrocystis pyrifera*).

The single-circular mitochondrial genome (mitogenome) of *P. usoehyunii* is composed 32,303 bp (Fig. S2), similar to other Dictyotales species (31,617–32,021 bp, Table 1). The mitogenome size in Dictyotales is smaller than in all other brown algal orders, including Ralfsiales and Ishigeales (Table 1). The GC content of the genes and intergenic space is, respectively, 35.40% and 40.24% (total GC content is 36.59%). The mitogenome has 75.43% gene density and conserved 36 PCGs, 25 tRNA genes, and 3 rRNA genes (Table S2), are commonly found in the mitogenomes of brown algae. Most of the mitogenomes have a core set of 35 genes, i.e., *atp6*, *atp8*, *atp9*, *cob*, *cox1*, *cox2*, *cox3*, *nad1*, *nad2*, *nad3*, *nad4*, *ad4L*, *nad5*,

nad6, *nad7*, *nad9*, *nad11*, *rpl2*, *rpl5*, *rpl6*, *rpl14*, *rpl16*, *rpl31*, *rps2*, *rps3*, *rps4*, *rps7*, *rps8*, *rps10*, *rps11*, *rps12*, *rps13*, *rps14*, *rps19* and *tatC*. Only one hypothetical protein was found in *P. usoehyunii*, located between *atp9* and *rpl16*. It is also found in the other two Dictyotales, which both contain two more hypothetical proteins. In *P. usoehyunii* only six genes (*rpl2*, *rps19*, *rps3*, *rpl16*, *ORF121*, and *tatC*) exist in the light strand with clockwise transcription direction (Fig. S2).

Phylogenetic assessment

Maximum Likelihood (ML) and Bayesian Inference (BI) trees were constructed using 115 and 35 common genes, respectively, from 27 chloroplast and 25 mitochondrial genomes (Table 1). The topologies of the ML and BI trees inferred from the chloroplasts and mitochondria genomes are highly congruent with maximum support values with the exception of the positions of the Desmarestiales and Fucales (Figs. 1 and 2). The chloroplast gene based tree showed the Dictyotales to be the sister to all other sampled orders (Fucophycidae) (Fig. 1), because Sphacelariales (a member of the Dictyophycidae) was assigned to the outgroup. Desmarestiales is sister to a clade comprising the other three orders in the Fucophycidae. The phylogenetic relationships based on chloroplasts genes are consistent with the results published by Bringloe et al. (2020) [10]. In contrast, in the mitochondrial gene-based tree, it is the Fucales that is sister to the other three fucophycidean orders (Fig. 2). Both organellar genomes demonstrated the monophyly of the Fucophycidae.

Structural variation in Phaeophyceae genomes

Synteny of organellar genome

The chloroplast co-linearity between *Padina usoehyunii* (Dictyotales) and other brown algal species can help to better visualize their comparative genomic structures. The circular diagrams (Fig. 3a) showed that the chloroplast genome of *P. usoehyunii* is highly lack of variation in structure when compared to the closely related *Dictyopteris divaricata* (Dictyotaceae, Dictyotales). A total of 36 co-linear blocks spanning 75,525 bp were identified, and no inversions were observed (Fig. 3a). In comparison to *Protohaloapteris* sp. (Sphacelariales), the co-linearity region covered 44,760 bp with 31 co-linear blocks and 19 identified inversion region (highlighted in gray, Fig. 3b) spanning 30,617 bp. The co-linearity between *P. usoehyunii* and *Desmarestia aculeata* (Desmarestiales) revealed 38 co-linear blocks covering 57,426 bp, which co-linear regions are smaller than that observed in *D. divaricata*, but larger than that of *Protohaloapteris* sp. (Fig. 3c). Additionally, nine inversion regions (13,665 bp in total length) were identified in *Desmarestia aculeata*. The co-linearity

Table 1 General features of organelle genomes in Phaeophyceae

Species	Order	Family	GenBank	Mitochondrion				Chloroplast				GenBank	CDs	tRNAs	rRNAs	ORF	Size(bp)
				CDs	tRNAs	rRNAs	ORF	CDs	tRNAs	rRNAs	ORF						
<i>Padina usoehtunii</i>	Dictyotales	Dictyotaceae	MW485979	36	25	3	1	32,303	MW485982	139	28	6	2	125,291			
<i>Dictyopteris divaricata</i>	Dictyotales	Dictyotaceae	NC_043845	38	24	3	3	32,021	NC_036804	139	27	6	2	126,099			
<i>Dictyota dichotoma</i>	Dictyotales	Dictyotaceae	NC_007685	38	24	3	3	31,617									
<i>Protohalopteris</i> sp.	Sphaecelariales	Styopocaulaceae	MZ156064 ^{a)}	39	23	n.d. ^{a)}	6	41,306	MZ156028	144	28	6	2	131,355			
<i>Desmarestia aculeata</i>	Desmarestiales	Desmarestiaceae	MZ156052	39	25	3	3	40,822	MZ156041	142	28	6	1	129,228			
<i>Desmarestia viridis</i>	Desmarestiales	Desmarestiaceae	NC_007684	39	25	3	4	39,049									
<i>Sargassum serratifolium</i>	Fucales	Sargassaceae	NC_066463	37	25	3	2	34,793	NC_066459	139	28	6	2	124,514			
<i>Sargassum macrocarpum</i>	Fucales	Sargassaceae	NC_066462	37	25	3	2	34,766	NC_066458	139	28	6	2	124,517			
<i>Sargassum fuivellum</i>	Fucales	Sargassaceae	NC_066461	37	25	3	2	34,763	NC_066457	139	28	6	2	124,277			
<i>Sargassum confusum</i>	Fucales	Sargassaceae	NC_066460	37	25	3	2	34,719	NC_066050	139	28	6	2	124,368			
<i>Sargassum siliquastrum</i>	Fucales	Sargassaceae	NC_050651	37	25	3	2	34,765	NC_064337	137	28	6	2	124,529			
<i>Sargassum fusiforme</i>	Fucales	Sargassaceae	MN883537	37	25	3	2	34,695	MN794016	139	28	6	2	124,298			
<i>Sargassum plagiophyllum</i>	Fucales	Sargassaceae	NC_064731	37	25	3	2	34,862	NC_064732	139	28	6	2	124,536			
<i>Sargassum polycystum</i>	Fucales	Sargassaceae	NC_064729	35	25	3	0	34,825	NC_064730	139	26	6	2	124,493			
<i>Sargassum hemiphyllyum</i>	Fucales	Sargassaceae	NC_024861	37	25	3	2	34,686	MT800998	139	28	6	2	124,319			
<i>Sargassum homeri</i>	Fucales	Sargassaceae	MH620963	37	24	3	2	34,621	NC_029856	139	28	6	2	124,068			
<i>Cocophora langsdorfi</i>	Fucales	Sargassaceae	NC_032287	37	25	3	2	35,660	NC_032288	139	27	6	2	124,450			
<i>Silvetia siliquosa</i>	Fucales	Fucaceae	MW485976	38	25	3	3	36,036	NC_061768	140	28	6	2	124,991			
<i>Fucus spiralis</i>	Fucales	Fucaceae	MG922856	37	25	3	2	36,396	MG922855	139	28	6	2	125,066			
<i>Chorda asiatica</i>	Laminariales s.l. ^{b)}	Chordaceae	MZ156050	40	25	3	5	41,788	MZ156037	141	28	6	0	130,274			
<i>Alaria marginata</i>	Laminariales	Alariaceae	NC_058764	38	25	3	3	39,389	NC_058769	141	29	6	0	130,582			
<i>Macrocystis pyrifera</i>	Laminariales	Laminariaceae	NC_065335	37	24	3	2	37,326	NC_065334	141	29	6	3	130,201			
<i>Saccharina japonica</i>	Laminariales	Laminariaceae	OP866273	38	26	3	3	37,657	OP866272	139	29	6	0	130,584			
<i>Laminaria ephemera</i>	Laminariales	Laminariaceae	MZ156055	38	25	3	3	37,929	MZ156035	142	29	6	1	130,610			
<i>Ectocarpus siliculosus</i>	Ectocarpales	Ectocarpaceae	MK045263	37	24	3	0	38,524	NC_013498	148	31	6	2	139,954			
<i>Enderacarne binghamiae</i>	Ectocarpales	Scytosiphonaceae	NC_036747	40	23	3	5	37,460	NC_038231	143	28	6	0	136,274			
<i>Scytosiphon lamentaria</i>	Ectocarpales	Scytosiphonaceae	NC_025240	39	25	3	4	36,918	NC_057081	137	27	6	3	134,485			

^{a)} Mitochondrial genome annotation of *Protohalopteris* sp. is incomplete

^{b)} In this study, we adopted the old classification of Laminariales. *Chorda asiatica* belonged to Laminariales

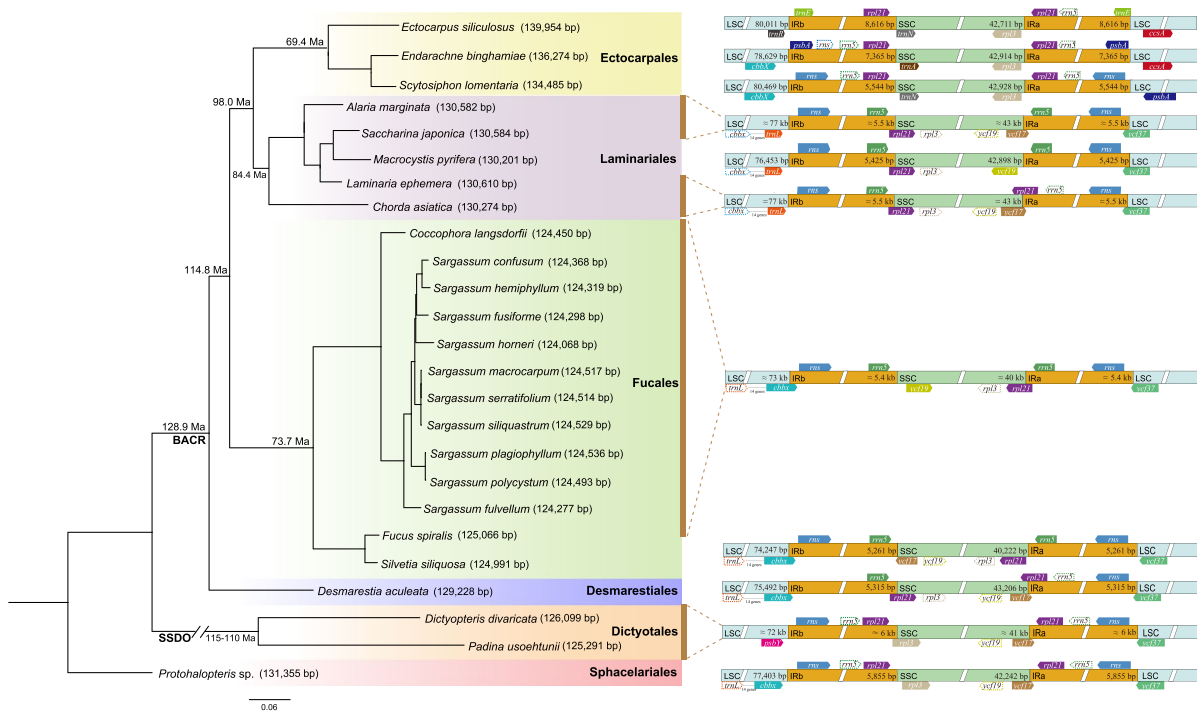


Fig. 1 Phylogenetic tree of brown algae (outgroup = Sphacelariales) constructed using the 115 shared chloroplast PCGs with IR, LSC, and SSC gene arrangement in boundary regions. The Maximum likelihood bootstrap support values and Bayesian posterior probabilities of all nodes are 100 and 1, respectively. The numbers before the tree nodes represent the mean divergence times retrieved from Silberfeld et al. (2010). Schematic representations of the chloroplast genomes for each taxon are shown right from the tree. Arrow icons of the same color represent the same genes, with arrow direction indicating the transcription orientation. Adjacent to boundary genes are represented by dashed line icons. The hash marks along the SSDO branch show that 1/3 length of the branch was cut for better visualization

between *P. usoehuntii* and five species within the order Fucales showed 29–37 co-linear blocks, spanning 37,748 to 51,710 bp (Fig. 3d, Fig. S3). Notably, the co-linear regions between *P. usoehuntii* and most species within the order Fucales consisted predominantly of inversion regions, ranging from 24,932 to 38,959 bp. Among them, *Silvetia siliquosa* (C.K.Tseng & C.F.Chang) E.A.Serrão, T.O.Cho, S.M.Boo & S.H.Brawley exhibited the highest proportion of inversion regions, accounting for 76% of the co-linear sequence. In comparison to five species within the order Laminariales, the co-linearity regions ranged from 47,115 to 52,827 bp, generally larger than those observed in Fucales (Fig. 3e, Fig. S3). However, the frequency of gene inversions was much lower, with only 2–5 inversion regions spanning 4,766 to 6,475 bp. When considering the co-linearity with Ectocarpaceales, *P. usoehuntii* shared the smallest co-linear regions of 39,764 bp to 47,461 bp, 17 inversion blocks covering 24,446 bp to 28,947 bp (Fig. 3f, Fig. S3).

Relative to the chloroplast genomes, the mitogenomes of brown algae are more conserved in structure (Fig. S4). Collinearity analysis of 12 brown algal mitogenomes showed that only Sphacelariales and Dictyotales

underwent rearrangement, and other brown algae exhibited highly conserved mitogenomes. Mitogenome rearrangement of Dictyotales occurred in a small region, with *P. usoehuntii* in the range of 10,400–10,950 bp and *Dictyopteris divaricata* in the range of 10,450–10,980 bp, and the gene *atp9* is located in these regions (Fig. S4). *Protohaloarteris* sp. contained two rearrangement regions (excluding incomplete annotations), one at 2,000–2,600 bp, with *nad3* and *rps14* in this region; the other at 14,000–16,000 bp, with *atp9* being identical to Dictyotales (Fig. S4).

Gene distribution in IR boundary region

Analysis of the IR boundary regions of 25 brown algal chloroplast genes revealed a high degree of conservation in the IR region: *rns*, *trnI*, *trnA*, *rnl*, *rrn5*, and *rpl21* (complete or partial). *Ectocarpus siliculosus* also includes *trnE*, *rpl32*, *trnL*, and *psbA* in its IR region (Fig. 1). However, the IR boundary regions exhibited different conservation levels. The boundary genes *rns* and *ycf37* of the IRa region and LSC region are the most conserved, except for the species of Ectocarpaceales. The boundary genes between LSC and IRb are *cbbx* and *rns* in Sphacelariales,

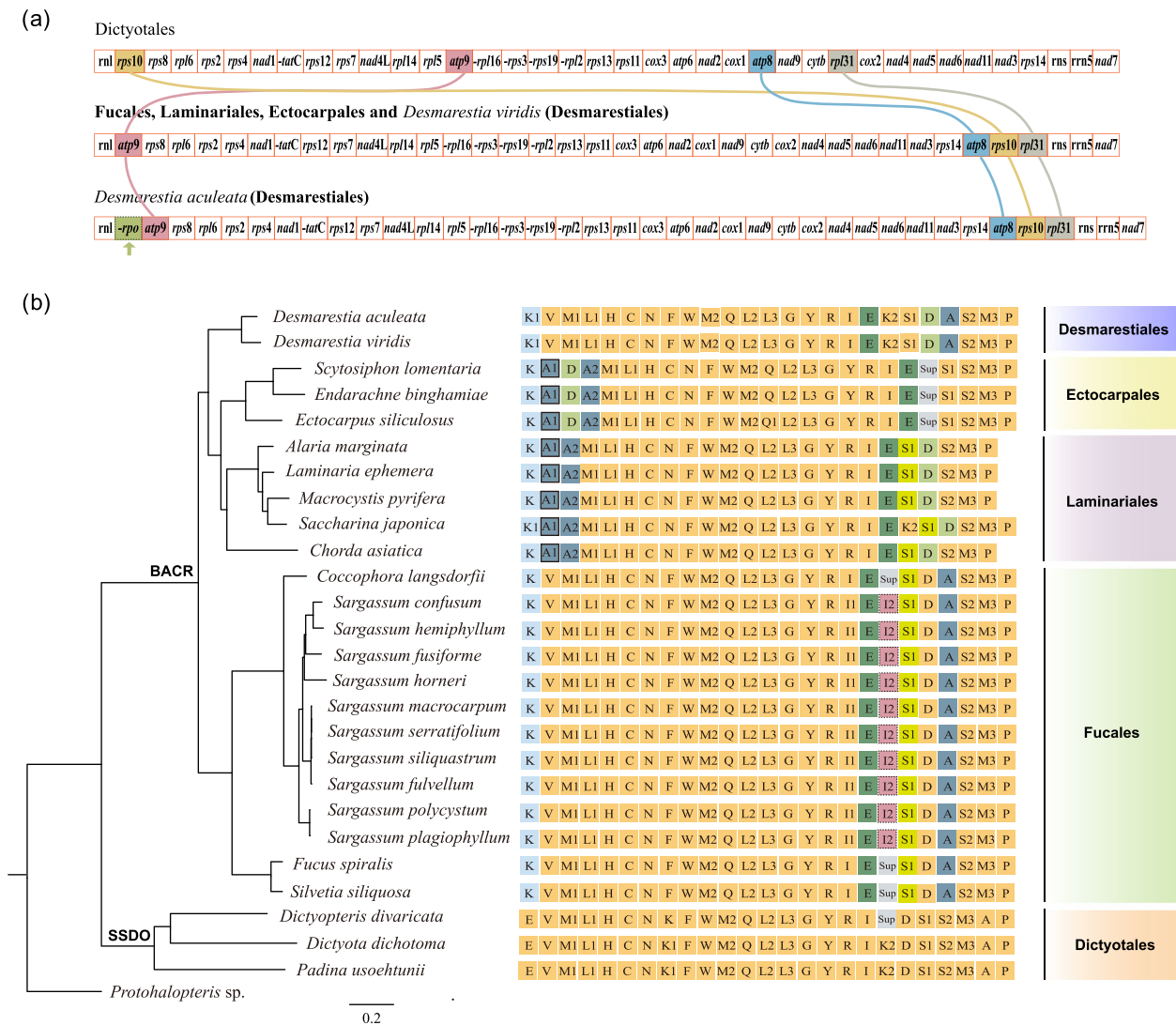


Fig. 2 Arrangement order of PCGs (a) and tRNAs (b) in mitochondrial genomes with the cladogram of brown algae constructed using the 35 shared mitochondrial PCGs. a: The gene arrangements in the mitogenome are marked using drawing collections among brown algal orders, and the *rpo* gene that uniquely occurs in *D. aculeata* is highlighted using a green arrow. b: Most nodes had high support values (Maximum likelihood bootstrap support values > 90 and Bayesian inference posterior probabilities > 95%), except for the marked numbers nodes. Using the *Padina usohtunii* mitogenome as reference (yellow squares), other color squares represent changed genes, dashed square represent inserted genes, solid squares represent replaced genes, and unframed squares represent genes with only changes in position. "Sub" represents predicted pseudogenes

Desmarestiales, Fucales and Ectocarpales (except for *E. siliculosus*), while *trnL* and *psbY* are found in species of Laminariales and Dictyotales (Fig. 1). The boundary genes *cbbx* in the Sphacelariales, Desmarestiales, and Fucales is interchangeable in genomic position with *trnL* in the Laminariales.

The inversion of the SSC region was observed in different orders of the Phaeophyceae. The boundary and adjacent genes of the IRa and SSC regions are *rpl21* and *rpl3* (IRa-SSC direction) in the Dictyotales, Desmarestiales,

Sphacelariales and Laminariales. The boundary and adjacent genes of IRb and SSC regions are *rpl21* (except for species of Laminariales which only have one *rpl21* in IRa-SSC) and *ycf17/ycf19*. Gene arrangement at the boundary of IRa-SSC and IRb-SSC regions is opposite to Ectocarpales and Fucales. Mauve collinearity analysis of chloroplast genomes of six brown algal orders showed that the entire SSC region of Dictyotales, Desmarestiales, Sphacelariales, and Laminariales species are inverted compared to those in Ectocarpales and Fucales (Fig. S5).

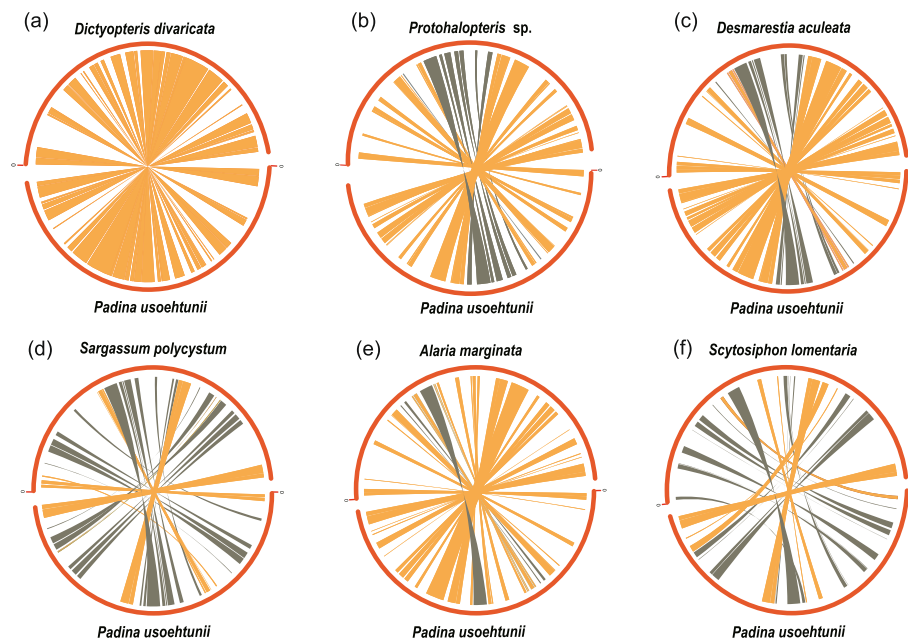


Fig. 3 Synteny circular diagrams comparing the chloroplast genome of *Padina usoehunii* with species from six brown algal orders. Orange represents collinear regions, and gray represents inverted collinear regions

Gene arrangement in mitogenome

The co-linearity analysis revealed the conserved nature of brown algal mitochondrial genome structures. The arrangement of core genes, including protein-coding genes (PCGs) and rRNA genes, showed that the mitochondrial PCGs consisted of the same set of 35 genes across all investigated species, except *Desmarestia aculeata* (Fig. 2a). Only four genes (*atp8*, *atp9*, *rps10*, *rpl31*) that primarily encode components involved in ATP synthesis and ribosomal proteins exhibited variations in order across different species, with a reference to a representative species from the order Dictyotales. Additionally, *Desmarestia aculeata* uniquely displayed an insertion of the *rpo* gene in the mitogenome compared to other brown algae (Fig. 2a). These findings indicate a high degree of conservation in the types and orders of PCGs in brown algal mitogenomes.

The number of tRNA genes ranged from 24 to 25 among the brown algae (Fig. 2b). Most species possessed 25 tRNA genes, with the lowest number found in Laminariales (Ectocarpales) except for *Saccharina japonica* (J.E.Areschoug) C.E.Lane, C.Mayes, Druehl & G.W.Saunders. Variations in tRNA gene arrangements were evident despite the relatively conserved numbers of tRNA genes. Using *Padina usoehunii* as a reference, the most common changes in tRNA gene positions occurred in *trnK*, *trnE*, *trnD*, *trnI* and *trnA*. Among them, the position change of *trnD* did not occur in Fucales, and the insertion of *trnI* only occurred in *Sargassum*. In

addition to the predicted pseudogenes, the position and order of tRNAs are conserved at the order level. A long tRNA block M1-L1-H-C-N-F-W-M2-Q-L2-L3-G-Y-R-I-E was found in all species of Fucoophycidae, indicating a highly conserved tRNA structure within the BACR clade. M1-L1-H-C-N and F-W-M2-Q-L2-L3-G-Y-R-I (two parts of the long tRNA block) occurred in all species within the Dictyotales.

Sequences variation in Phaeophyceae genomes

Base evolutionary rate

Non-synonymous (dN) and synonymous (dS) substitution rates across 24 brown algal species encompassing five orders (Tables S3-S4) can help to understand sequence variations of chloroplast and mitochondrial common PCGs. Among the 115 chloroplast genes, the highest dN value was observed in *rps20* (0.3385), while the lowest values were found in *petN* and *psbL* (0.0001). The photosystem II genes *psbA*, *psbE*, and *psbK* exhibited the lowest dS (0.3506–0.3770) and relatively small dN values (0.0138–0.0518). The dN/dS ratios were smallest for *petN* (0.0001 < 1) and *psbL* (0.0002 < 1) (Fig. S6a), indicating an intense signature of purifying selection. Conversely, the genes *petF* and *rpl9* displayed the highest dN/dS ratios (0.4401 < 1, 0.3960 < 1), indicating a weak purifying selection.

The functional gene category ribosomal proteins exhibited significant differences in dN/dS ratios compared to genes involved in photosystem, light harvesting and

chlorophyll biosynthesis ($p=0.001$, $p=0.009$) (Fig. 4a). The highest average dN/dS ratio (0.1595) in ribosomal proteins indicates a much weak evolutionary pressure. The lowest average dN/dS ratios (0.0626, 0.0632) detected in genes involved in light harvesting, chlorophyll biosynthesis and photosystem categories suggest the strongest signature of purifying selection.

Among the 35 mitochondrial genes, the highest dN/dS ratio occurred in ribosomal protein genes: *rpl5* (0.2825), *rps10* (0.2853), *rps11* (0.2952), *rps2* (0.3071), and *rpl31* (0.4309) (Fig. S6b, Table S4), suggesting their relatively accelerated evolutionary rates. The lowest ratio was found in *atp9* (0.0168). The dN/dS ratios for four functional groups in mitogenome (ATP synthase, cytochrome c oxidase, NADH dehydrogenase and ribosomal proteins) (Fig. 4b), detected significantly high values in ribosomal protein genes compared to cytochrome c oxidase ($p=0.009$) and NADH dehydrogenase genes ($p=0.001$).

Significant differences in dN and dS values were observed between the mitochondrial genes and chloroplast genomes of brown algae ($p=0.001$). The dN values of chloroplast genes ranged from 0.0001 to 0.3385, whereas those of mitochondria ranged from 0.0062 to 0.4213 (Tables S3-S4). The dS values of chloroplast genes ranged from 0.3506 to 1.1051, whereas the mitochondrial ones ranged from 0.9423 to 2.0364 (except *atp9*, dS=0.3697). Most mitochondrial genes generally showed higher dS and dN values than the chloroplast genes (Fig. 5), indicating that mitochondrial genes had higher

mutation rates than the chloroplast genes in brown algae. The dN/dS values of chloroplast genes ranged from 0.0098 to 0.4401 (except *petN* (dN/dS=0.0001) and *psbL* (dN/dS=0.0002)) and those of mitochondrial genes ranged from 0.0168 to 0.4309 (Fig. S6). This statistically non-significant difference ($p=0.724$) manifests that they both experienced potential purifying selection at similar levels.

Codon usage

RSCU values revealed the use preferences of 61 codons (excluding three stop codons) in brown algae. AUU was the most frequent codon for Leu in chloroplast and mitochondrial genomes. Approximately 25–27 codons (RSCU>1) were preferred in organellar genomes. RSCU>1.6 is considered as over-preference for codons, while RSCU<0.6 expresses that codons are under-preferred [29]. Accordingly, 13 codons were identified as frequently used codons (RSCU>1.6, average RSCU=2.00) whereas 27 codons were underused (RSCU<0.6, average RSCU=0.28) in chloroplast genomes (Fig. S7). In mitogenomes, there were four over-preferred codons (RSCU>1.6, average RSCU=2.26) and eight under-preferred codons (RSCU<0.6, average RSCU=0.30) (Fig. S8). The codon bias of the chloroplast genome is stronger than that of the mitogenome in brown algae and the third position of frequently used codons was predominantly A or U.

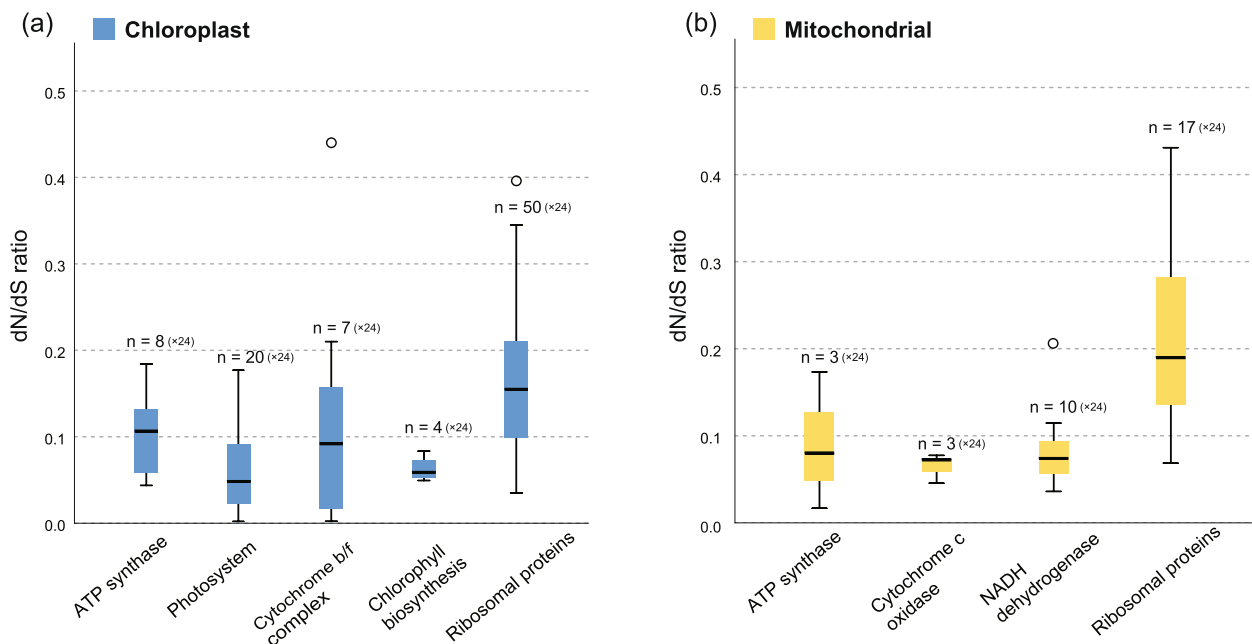


Fig. 4 Boxplots of dN/dS values of major functional group of genes in chloroplasts (a) and mitochondria (b) of 24 brown algae. “n” represents the number of genes in each functional group

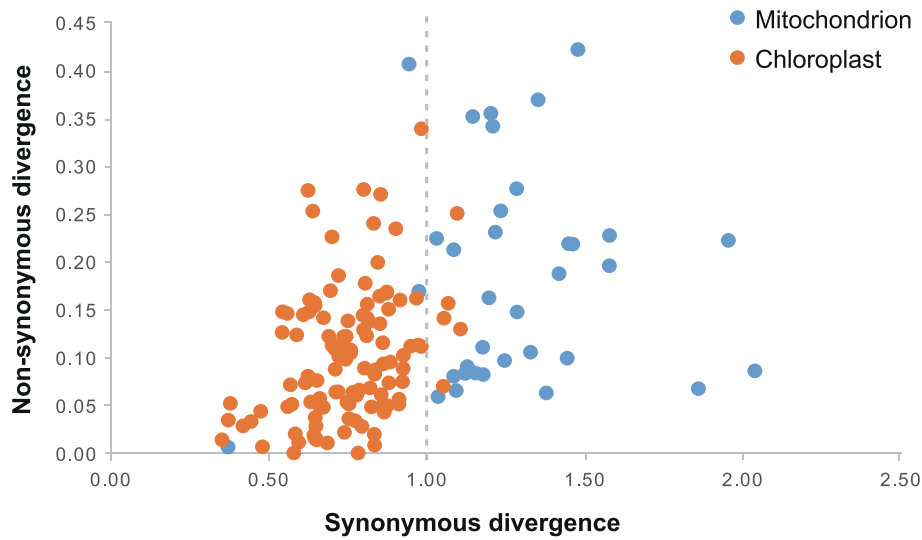


Fig. 5 Non-synonymous (dN) and synonymous (dS) substitution rates for 115 chloroplast common PCGs (orange dots) and 35 mitochondrial common PCGs (blue dots) across 24 brown algae

Repeat sequences

A total of 105 (*Padina usoehuntii*) to 157 (*Chorda asiatica* Sasaki & Kawai) simple sequence repeats (SSRs) were detected in 14 chloroplast genomes, including 81–113 mononucleotides (mono-), 4–16 dinucleotides (di-), 3–13 trinucleotides (tri-), 4–15 tetranucleotides (tetra-), 0–5 pentanucleotide (penta-), and 0–2 hexanucleotide (hexa-) (Fig. S9). In 14 mitogenomes analyzed, there are 22 (*P. usoehuntii*) to 52 (*E. siliculosus* and *Scytosiphon lomentaria* (Lyngbye) Link) SSRs, and the numbers of mono-, di-, tri-, tetra-, penta-, and hexa-nucleotide are 20–47, 0–3, 0–2, 0–4, 0–1, 0–1, respectively (Fig. S9). The most numerous mononucleotides repeats are of the A and T type. *P. usoehuntii* had the least numbers of SSRs among brown algae. We identified the forward (F), reverse (R), palindromic (P), and complementary (C) repeat sequences in chloroplast and mitochondrial

genomes of brown algae (Fig. 6). Palindromic repeats are the most frequent in chloroplast genomes, while forward repeats are the most frequent type in mitogenomes. Complementary repeats are the least frequent type in both organelle genomes. The amount of these long repeat sequences was highly variable in mitogenomes, with 38 forward repeats and 6 palindromic repeats in *Protohalopteris* sp., 20 forward repeats and 15 palindromic repeats in *P. usoehuntii*. In chloroplast genomes, the numbers of different repeat types is more conserved within the same brown algal order.

Discussion

When codon bias, number and types of repeat sequences, and particularly genome size and structure, were mapped on the phylogenetic tree of the Phaeophyceae, varying degrees of diversity at the order level became apparent

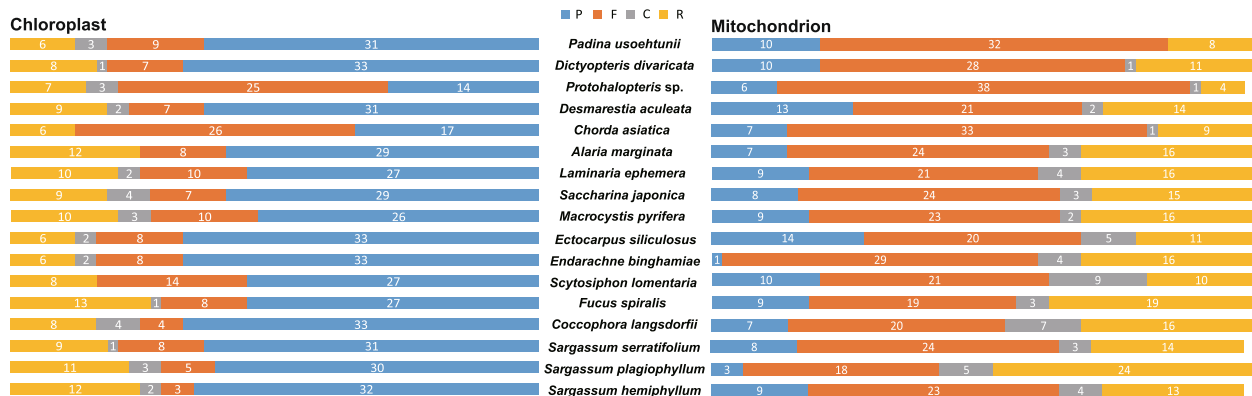


Fig. 6 Numbers of different repeated sequence types in organellar genomes of the Phaeophyceae species

(Fig. S1-S2). The structural differences in chloroplast genome primarily reflected on the size and types of genes at the IR boundary region and the rearrangement of the SSC region, which may mechanically be related to gene replication. In brown algae, chloroplast genomes are more variable in structure, while mitochondrial genomes exhibit higher sequence variation. This pattern is similar in red algae [30, 31], but contrasts that in land plants and green algae [18, 32]. The rate of sequence evolution is likely influenced by the extent of organellar genome modification as observed in terrestrial plants [33].

Organelle genome size and gene loss

The Dictyotales with divergence time around 155 Ma [5] has a smaller chloroplast genome size, compared to the late-diverged lineages within the BACR clade, except Fucales (Fig. 1), which has a similar chloroplast genome size as Dictyotales (around 125 kb). Previous researches showed a positive correlation between chloroplast genome size and the total length of non-coding sequences in the subclass Fucophycidae [34], suggesting that the accumulation of non-coding regions contributes to larger chloroplast genomes. There are possibly significant positive correlations between the chloroplast genomes in the brown algal SSDO-BACR clades and the total length of non-coding sequences, indicating that non-coding sequences possibly contributed to the emergence of new chloroplast genes.

In comparison with other orders of Phaeophyceae, Dictyotales exhibits distinctive gene losses in its chloroplast genome: *rbcR* and *rpl32* (Fig. S1). *rbcR* is a potential transcriptional regulator of Rubisco and its absence has not been observed in other brown algal lineages. Endosymbiotic gene transfer likely occurred between the organelles and the nucleus in Dictyotales, leading to the presence of *rbcR* in the nucleus [35]. This hypothesis requires further validation in some targeted taxa (e.g. Syringodermatales and Sphacelariales) that are phylogenetically close to Dictyotales [5]. *rpl32* has been found to be lost in 21 algal chloroplast genomes, mostly belonging to the Streptophyta, like some seed plants: eudicots, gymnosperms, magnoliids, and monocots [36]. Gene loss events within chloroplast genomes have been observed in other Ochrophyta lineages such as Dictyochophyceae and Synurophyceae [37, 38], suggesting that these gene loss events are not uncommon during the course of evolution. However, it is not clear that is gene loss or transfer responsible for the absence of *rbcR*. The absence of *rbcR* and *rpl32* genes happened after the SSDO-BACR split, because secondary gain of these genes in the BACR clade is highly unlikely. We do not know whether these genes were lost early during SSDO evolution or whether it happened

later, because no SSDO chloroplasts other than those from the Dictyotales have been sequenced.

Variation of organelle genome structure

Structural comparison of chloroplast genomes between *Padina usoehtunii* and other orders revealed clear differences across the phylogenetic tree of brown algae. The BACR orders Laminariales, Fucales, and Desmarestiales showed large structural differences compared to Dictyotales in chloroplast genome organization (Fig. S3). Notably, Dictyotales displayed a smaller number of inverted regions compared to the Laminariales than to the Fucales and Ectocarpales (Fig. S3). A certain degree of chloroplast genome structural instability can generate adaptive and recovery mechanisms to cope with environmental changes, accelerating the evolutionary trajectory of brown algae and aiding their expansion into a wide range of geographical environments [39].

The IR region is crucial in terrestrial plants as it stabilizes chloroplast genome organization, mediates intramolecular recombination, and increases the copy number of rRNA genes [40]. The expansion and contraction of the IR region are linked to the addition or reduction of boundary genes (Fig. 1). The size of the IR region varies significantly among different Ochrophyta algae, such as Raphidophyceae and Bacillariophyceae, which have IR sizes of 18–22 kb, approximately three times larger than that in brown algae (5–9 kb). The IR region in brown algae includes rRNA and tRNA genes, while in the Raphidophyceae and Bacillariophyceae it also contains ribosomal protein genes such as *rpl32*, *rpl21*, *rpl34*, as well as photosystem II genes *psbA*, *psbY*, and *psbC* [41, 42]. The IR region structure in oogamous (with maternal chloroplast inheritance) Dictyotales, Laminariales, and Fucales, is relatively conserved, while substantial structural variation is observed among different species of isogamous Ectocarpales (with biparental chloroplast inheritance), which accumulate more variation compared to oogamous brown algae, leading to a higher rate of structural rearrangements [34].

rpl21 is a common gene between the IR and SSC boundary regions in brown algae. The contraction or expansion of the IR region can affect the location of *rpl21* (Fig. 1). When the IR region is large, the *rpl21* gene and its replicates are present in the IRa and IRb, as in the Dictyotales (IR: 5.8–6 kb), Sphacelariales (IR: 5.9 kb), and Ectocarpales (IR: 7.3–8.6 kb). As an exception, *S. lomentaria* (Ectocarpales) possessed a complete *rpl21* with a relatively small IR region (5.5 kb). When the IR region is small, *rpl21* will span the IR and SSC regions, as in the Desmarestiales (IR: 5.3 kb), Fucales (IR: 5.2–5.4 kb) and Laminariales (IR: 5.4–5.5 kb). The inversion of the entire SSC region happened two times,

the first occurred between 144.6–54.6 Ma, after the split of the Fucales from the Desmarestiales, and the second occurred between 125.0–51.5 Ma, after the split of the Ectocarpales from the Laminariales. (Fig. S5) [5]. Such an inversion has been found in many plant taxa, such as *Centaurea diffusa* (Asteraceae) [43], *Phaseolus vulgaris* (Fabaceae) [44] and *Buxus microphylla* (Buxaceae) [45]. Recombination within the reverse repeat can lead to polarity reversal in the SSC region that appears to occur frequently in the chloroplast genome [44]. Mechanistically, this recombination may be related to the content of G + C [46] and the presence of tRNA in the IR region [47] in which high G + C content is more prone to mutation [48].

Phylogenetic analysis showed that the *cbbx* gene originated in cyanobacteria [35]. The CbbX protein can function as an activase of inhibited red-type Rubisco [49]. Bi et al. (2000) found that *cbbx* in the brown alga *Saccarina japonica* exists in the nuclear and in the chloroplast genome [49]. The nuclear-encoded *cbbx* (*cbbx-n*) exhibits higher enzyme activity compared to the plastid-encoded *cbbx* (*cbbx-p*). *cbbx-n* can interact with *cbbx-p* to form a heterohexamer, promoting higher catalytic efficiency of Rubisco, thereby accelerating the rate of carbon assimilation in photosynthesis [49]. The rearrangements of the *cbbx* gene in certain brown algal lineages may affect the catalyzing efficiency of Rubisco, thus influencing the rate of carbon assimilation in photosynthesis. However, this hypothesis requires further experimental validation.

Variation of organellar genome sequence

We found a significantly higher non-synonymous (dN) substitution rate in mitochondrial genes compared to chloroplast genes, which is consistent with the previous research on the evolutionary rate in brown algae [18]. The average synonymous (dS) substitution rate in mitochondria is higher than in chloroplasts, although this distinction is not clearly discernible in the scatterplot in Fig. 5. This observation may be attributed to the inclusion of Dictyotales and Sphacelariales. Nevertheless, when considering the entire organellar genome dataset, it is evident that brown algal mitochondrial genes have a faster mutation rate than chloroplasts genes (Tables S3–S4). This was also observed in the phytoplankton *Phaeocystis* (Haptophyta) and the red alga *Porphyra* [50, 51], but this trend was in contrast to most land plants, where the dS value of mitochondria were three times lower than the chloroplasts [52].

For both chloroplast and mitochondrial genomes, the average dN/dS values for all protein coding genes (PCGs) are less than 1, suggesting that these genes have undergone potential purifying selection. However,

genes from different functional categories showed variable dN/dS values. Notably, the ribosomal protein genes, whether in chloroplasts or in mitochondria, exhibited the highest average dN/dS values, suggesting much weaker signature of purifying selection. In the chloroplast genomes, the strongest signature of purifying selection is observed in the photosystem genes, consistent with the predicted dN/dS values for the primary functional groups of 23 brown algal species reported recently [18]. These differences of the dN/dS values with different function genes reflected variation in the strength of purifying selection.

Highly preferred codons in both chloroplast and mitochondrial genomes all ended with A/U, while less preferred codons ended with C/G (Figs. S7–S8). Codon preference analysis indicates that codon usage patterns are similar among different brown algal species. However, codon bias in the brown algal chloroplast genome is higher than in the mitochondrial genome. Selective pressure and gene mutations are likely important factors to influence codon usage [53], possibly due to the high AT content in organellar genomes which can potentially lead to a bias towards AU in codons. In sum, this study confirmed some early observed essential findings such as the more prevalent structural inversions across chloroplast genomes than mitochondria, though mitochondrial genes evolved at a faster rate than chloroplast. Boundary genes, particularly their positions and the changes in the number, likely contributed to the IR regions in chloroplast genome and hence accounted for the gain or loss of chloroplast genes. These results, together with other sequenced and sequencing organellar genomes can substantially improve our understanding of phylogenetic diversity and molecular evolution of the brown algal tree of life.

Materials and methods

Sample collection and DNA extraction

Padina usoehtunii was collected from the intertidal at Pakarang Cape (8°44′17.9″N 98°13′05.5″E) in Phangnga province on the Andaman coast of Thailand in December 2019, silica-dried and transported to Qingdao, China. Species identification was a posteriori confirmed by comparing mitochondrial *cox3* and chloroplast-encoded *rbcl* gene sequences to the representative DNA sequences of the *P. usoehtunii* type specimen (Genbank AB512597 and AB512559, respectively). The total DNA was extracted from young thallus using the FastPure® Plant DNA Isolation Mini Kit (Vazyme Biotech Co., China). The extracted DNA was purified using a DNA Purification Kit (Vazyme Biotech Co., China) according to manufacturer's instructions.

Genome sequencing, assembly and annotation

To obtain full-length chloroplast and mitochondria genome sequences, we used the paired-end (Illumina HiSeq) strategy in this study. First, approximately 1 µg of purified DNA was made into libraries using the TruSeq™ Nano DNA Sample Prep Kit from Illumina according to the manufacturer's protocol. Libraries were sequenced using an Illumina HiSeq 4000 with 150 bp paired-end reads length (Biozeron, Shanghai, China). The raw reads (ca. 8.9×10^8) were checked with FastQC and trimmed by Trimmomatic-0.39 [54]. Algal organellar genomes assembly was performed using NOVOPlasty v2.7.2 software (<https://github.com/ndierckx/NOVOPlasty>). The near-source reference genome was used as the seed sequence, with the remaining parameters set as default. Clean reads ($10^5/1.3 \times 10^5$ Mb) were compared back on the Scaffold obtained by assembly, and based on the paired-end and overlap of reads, the assembly results were partially assembled and optimized. GapCloser v1.12 (<http://soap.genomics.org.cn/soapdenovo.html>) was used to repair the internal holes in the assembly.

The mitochondrial and chloroplast genes were annotated using the online GeSeq tool (<https://chlorobox.mpimp-golm.mpg.de/geseq.html>) to predict protein coding genes, ORFs, tRNA and rRNA, using following parameters: Protein search identity: 60; rRNA, tRNA, DNA search identity: 35; 3rd Party tRNA annotators: tRNAscan-SE. The position of each coding gene was determined using BLAST [55] searches against reference genes. Manual corrections of genes for start/stop codons and for intron/exon boundaries were performed in SnapGene Viewer. The circular maps of genomes were displayed using the software OGDRAW (<https://chlorobox.mpimp-golm.mpg.de/OGDraw.html>). Gene function annotation was performed with available protein databases by BLASTp (evalue $\leq 10^{-5}$), including NCBI Non-Redundant Protein Sequence Database (NR), Swiss-Prot, Clusters of Orthologous Groups (COGs), and Kyoto Encyclopedia of Genes and Genomes (KEGG) and Gene Ontology (GO) terms. Finally, we submitted the mitochondrial and chloroplast genomes of *Padina usoehtunii* to the GenBank database with accession numbers MW485979 and MW485982, respectively.

Phylogenetic analysis

We selected 27 and 25 species from 6 orders of Phaeophyceae (Table 1) to construct mitochondrial and chloroplast phylogenetic trees respectively, using *Protohalopectis* sp. (Sphacelariales) as outgroup. Sequences of 35 and 115 shared genes from mitogenomes and chloroplast genomes were aligned by mafft v7.313 [56] and the sequences were removed highly divergent or ambiguously aligned sites with Gblock 0.91b [57]. IQtree

v.1.6.8 [58–60] and MrBayes 3.2.6 [61] were used to construct Maximum likelihood (ML) and Bayesian inference (BI) trees, respectively. ModelFinder [62] was used to select the best nucleotide substitution model based on Akaike information criterion (AIC). The best-fit models GTR+F+I+G4 (G=0.232, I=0.800) and GTR+F+I+G4 (G=0.352, I=0.853) were used for mitochondria and chloroplast, respectively. For ML tree construction, the parameters were set to 1000 ultrafast bootstrap replicates with others as default [60]. For BI tree, the Markov Chain Monte Carlo (MCMC) were set to 1×10^6 generations running with a tree sampling frequency of every 1000 generations and the first 25% was discarded as burn-in. Finally, FigTree v1.4.4 (<http://tree.bio.ed.ac.uk/software/figtree>) was used to beautify the tree files.

Genome synteny and gene arrangement analysis

We used TBtools v1.108 to map the collinearity of chloroplast genome structure between *P. usoehtunii* and six species from the Dictyotales, Sphacelariales, Desmarestiales, Laminariales, Ectocarpales, and Fucales, respectively [63]. The species annotation order was manually adjusted to be consistent to ensure correct collinear correspondence. BLAST [55] was used to match synteny, sequences with less than 100 bp were removed, and only a pair of IR collinear information (IRa-IRa, IRb-IRb) was retained. Mauve [64] was used to detect linear collinearity of chloroplast genomes, setting to align with progressive Mauve. In order to explore the differences of chloroplast LSC/IR/SSC region boundaries, we plotted the genes between each partition by CPJSDraw v1.0.0 [65]. tRNAscan-SE v.2.0 [66] was used to predict the number and location of tRNAs in the gene order of all mitogenomes.

Base substitution rate estimation

To explore evolutionary rates of brown algal organelle genomes, we extracted 35 and 115 shared PCGs from 24 species whose both organelles have been sequenced using PhyloSuite v1.2.2 [67]. The genome datasets of Phaeophyceae were obtained from GenBank (Table 1). MAFFT [56] and Gblocks [57] were used for sequence alignment and correction, respectively. The aligned sequence was converted into pml format by PhyloSuite v1.2.2 [67]. We used PAML v4.10 [68] to estimate non-synonymous (dN) and synonymous substitution (dS) of 24 mitogenomes and chloroplast genomes. The parameters set to runmode=0 and CodonFreq=2. To avoid data bias we calculated the median pairwise comparisons data of each gene. The histogram was drawn to show dN/dS values of each gene. The scatter plot was drawn to show the tendency of differences in dN/dS

values among chloroplasts and mitochondria. We used the Kruskal–Wallis test in SPSS v26.0 software (IBM, Armonk, NY, USA) to explore the diversity in dN/dS values of different functional genes. The comparison of substitution rate between the two organelles was also tested using the method above.

Repeat sequences and codon preference analysis

Short Sequence Repeats (SSRs) were identified using MISA [69]. The parameter settings were as follows: mono-, di-, tri-, tetra-, pent-, and hexa-nucleotide motifs have at least 8, 5, 4, 3, 3 and 3 repeats, respectively. We used REPuter (<http://bibiserv.techfak.uni-bielefeld.de/reputer>) to detect forward (F), palindromic (P), reverse (R) and complementary (C) repeats with Hamming distance equal to 3 and minimum repeat size of 20 bp [70]. The PCGs of organelles were extracted by PhyloSuite v1.2.2 [67]. CodonW v1.4.4 [71] was used to calculate the relative synonymous codon usage (RSCU) of each PCGs. RSCU = 1 means no bias in codon usage. RSCU < 1 indicates less codon usage, while RSCU > 1 shows more preference in codon usage [72].

Abbreviations

AIC	Akaike information criterion
BACR	Brown algal crown radiation
BI	Bayesian inference
<i>cbx-n</i>	Nuclear-encoded <i>cbx</i>
<i>cbx-p</i>	Plastid-encoded <i>cbx</i>
COGs	Clusters of Orthologous Groups
dN	Non-synonymous substitution
dS	Synonymous substitution
GO	Gene Ontology
IR	Inverted repeat
ITS	Internal transcribed spacer
KEGG	Kyoto Encyclopedia of Genes and Genomes
LSC	Long single copy
Ma	Mega-annum
MCMC	Markov Chain Monte Carlo
ML	Maximum likelihood
NR	Non-Redundant Protein Sequence Database
PCGs	Protein coding genes
RDR	Recombination-dependent replication
rRNAs	Ribosomal RNA genes
SSC	Short single copy
SSDO	Sphacelariales, Syringodermatales, Dictyotales, and Onslowiales
tRNAs	Transfer RNA genes

Supplementary Information

The online version contains supplementary material available at <https://doi.org/10.1186/s12864-024-10616-4>.

Supplementary Material 1.
Supplementary Material 2.
Supplementary Material 3.
Supplementary Material 4.
Supplementary Material 5.

Acknowledgements

We are grateful for the joint support from the National Natural Science Foundation of China (32371697), the National Natural Science Foundation of China (41761144057) and the Thailand Research Fund (RDG6130002).

Sample collection permission

The collection of algae samples in this article complied with Thailand legislation and international guidelines.

Authors' contributions

Z.M. Hu and S.G.A. Draisma led this project. Y.J. Liu, T.Y. Zhang and Q.Q. Wang collectively conducted the experiments and performed data analysis. Y.J. Liu drafted the manuscript. Z.M. Hu provides important advice on writing. S.G.A. Draisma collected the samples and revised the manuscript. All authors approved the final version of the manuscript for publication.

Funding

This work was supported by National Natural Science Foundation of China (32371697), a joint research grant between National Natural Science Foundation of China (41761144057) and Thailand Research Fund (RDG6130002).

Availability of data and materials

The GenBank accession numbers of the chloroplast and mitochondrial genomes of *Padina usoehunii* are MW485982 and MW485979, respectively.

Declarations

Ethics approval and consent to participate

Not applicable.

Consent for publication

Not applicable.

Competing interests

The authors declare no competing interests.

Author details

¹Ocean School, Yantai University, Yantai 264005, China. ²Excellence Center for Biodiversity of Peninsular Thailand, Faculty of Science, Prince of Songkla University, Hat Yai, Songkhla 90110, Thailand.

Received: 5 January 2024 Accepted: 12 July 2024

Published online: 31 July 2024

References

- Kurland CG, Andersson SG. Origin and evolution of the mitochondrial proteome. *Microbiol Mol Biol Rev.* 2000;64(4):786–820.
- Kutschera U, Niklas KJ. Endosymbiosis, cell evolution, and speciation. *Theory Biosci.* 2005;124(1):1–24.
- Brindefalk B, Ettema TJ, Viklund J, Thollesson M, Andersson SG. A phylometagenomic exploration of oceanic alphaproteobacteria reveals mitochondrial relatives unrelated to the SAR11 clade. *PLoS ONE.* 2011;6(9):e24457.
- Cock JM, Sterck L, Rouzé P, Scornet D, Allen AE, Amoutzias G, et al. The *Ectocarpus* genome and the independent evolution of multicellularity in brown algae. *Nature.* 2010;465:617–21.
- Silberfeld T, Leigh JW, Verbruggen H, Cruaud C, de Reviers B, Rousseau F. A multi-locus time-calibrated phylogeny of the brown algae (Heterokonta, Ochrophyta, Phaeophyceae): Investigating the evolutionary nature of the “brown algal crown radiation.” *Mol Phylogenet Evol.* 2010;56(2):659–74.
- Rajanikanth A. A fossil marine brown alga from the Gangapur Formation. Pranhita-Godavari Graben *Curr Sci.* 1989;58(2):78–80.
- Parker BC, Dawson EY. Non-calcareous marine algae from California Miocene deposits. *Nova Hedwigia Beihefte.* 1965;10:273–95.
- Reviere BD, Rousseau F. Towards a new classification of the brown algae. *Phycol Res.* 1999;13(1):107–201.

9. Draisma SGA, Prud'homme van Reine WF, Stam WT, Olsen JL. A reassessment of phylogenetic relationships within the phaeophyceae based on rubisco large subunit and ribosomal DNA sequences. *J Phycol.* 2001;37(4):586–603.
10. Bringloe TT, Starko S, Wade RM, Vieira C, Kawai H, Clerck OD, et al. Phylogeny and evolution of the brown algae. *Crit Rev Plant Sci.* 2020;39(4):281–321.
11. Wei L, Xin Y, Wang D, Jing X, Zhou Q, Su X, et al. *Nannochloropsis* plastid and mitochondrial phylogenomes reveal organelle diversification mechanism and intragenus phylotyping strategy in microalgae. *BMC Genomics.* 2013;14:534.
12. Muhlin JF, Brawley SH. Recent versus relic: discerning the genetic signature of *Fucus vesiculosus* (Heterokontophyta; Phaeophyceae) in the Northwestern Atlantic. *J Phycol.* 2009;45(4):828–37.
13. Hu ZM, Uwai S, Yu SH, Komatsu T, Duan DL. Phylogeographic heterogeneity of the brown macroalga *Sargassum horneri* (Fucaceae) in the north-western Pacific in relation to late Pleistocene glaciation and tectonic configurations. *Mol Ecol.* 2011;20(18):3894–909.
14. Hu ZM, Kantachumpoo A, Liu RY, Sun ZM, Yao JT, Komatsu T, Uwai S, Duan DL. A late Pleistocene marine glacial refugium in the south-west of Hainan Island, China: phylogeographical insights from the brown alga *Sargassum polycystum*. *J Biogeogr.* 2018;45:355–66.
15. Li JJ, Hu ZM, Sun ZM, Yao JT, Liu FL, Fresia P, Duan DL. Historical isolation and contemporary gene flow drive population diversity of the brown alga *Sargassum thunbergii* along the coast of China. *BMC Evol Biol.* 2017;17:246.
16. Montecinos AE, Couceiro L, Peters AF, Desrut A, Valero M, Guillemelin ML. Species delimitation and phylogeographic analyses in the *Ectocarpus* subgroup *siliculosi* (Ectocarpales, Phaeophyceae). *J Phycol.* 2017;53(1):17–31.
17. Chen J, Zang Y, Liang S, Xue S, Shang S, Zhu M, et al. Comparative analysis of mitochondrial genomes reveals marine adaptation in seagrasses. *BMC Genomics.* 2022;23(1):800.
18. Starko S, Bringloe TT, Gomez MS, Darby H, Graham SW, Martone PT. Genomic rearrangements and sequence evolution across brown algal organelles. *Genome Biol Evol.* 2021;13(7):evab124.
19. Liu F, Pan J, Zhang Z, Zhang ZS, Moejeset FW. Organelle genomes of *Sargassum confusum* (Fuciales, Phaeophyceae): mtDNA vs cpDNA. *J Appl Phycol.* 2018;30:2715–22.
20. Zhang SS, Liang YS, Zhang J, Draisma SGA, Duan D. Organelle genome comparisons of *Sargassum polycystum* and *S. plagiophyllum* (Fuciales, Phaeophyceae) with other *Sargassum* species. *BMC Genomics.* 2022;23(1):629.
21. Liu F, Zhang Y, Bi Y, Chen W, Moejeset FW. Understanding the evolution of mitochondrial genomes in Phaeophyceae inferred from mitogenomes of *Ishige okamurai* (Ishigeales) and *Dictyopteris divaricata* (Dictyotales). *J Mol Evol.* 2019;87(1):16–26.
22. Liu F, Jin Z, Wang Y, Bi Y, Melton JT 3rd. Plastid genome of *Dictyopteris divaricata* (Dictyotales, Phaeophyceae): Understanding the evolution of plastid genomes in brown algae. *Mar Biotechnol.* 2017;19(6):627–37.
23. Vieira C, Steen F, D'hondt S, Bafort Q, Tyberghein L, Fernandez-García C, et al. Global biogeography and diversification of a group of brown seaweeds (Phaeophyceae) driven by clade-specific evolutionary processes. *J Biogeogr.* 2021;48:703–15.
24. Vieira C, Camacho O, Sun Z, Fredericq S, Leliaert F, Payri C, et al. Historical biogeography of the highly diverse brown seaweed *Lobophora* (Dictyotales, Phaeophyceae). *Mol Phylogenet Evol.* 2017;110:81–92.
25. Guiry MD, Guiry GM. 2023. AlgaeBase. World-wide electronic publication, National University of Ireland, Galway. <https://www.algaebase.org>; searched on December 22, 2023.
26. Ni-Ni-Win, Hanyuda T, Arai S, Uchimura M, Prathep A, Draisma SGA, et al. A taxonomic study of the genus *Padina* (Dictyotales, Phaeophyceae) including the descriptions of four new species from Japan, Hawaii, and the Andaman sea. *J Phycol.* 2011;47(5):1193–1209.
27. Wichachucherd B, Prathep A. Preliminary study on the diversity and distribution of *Padina* Adanson in Peninsular Thailand, including a new record, *Padina useohtunii* Ni-Ni-Win et Kawai. Institute of Ocean and Earth Sciences University of Malaya Monograph. 2013;15:175–83.
28. Wichachucherd B. Phylogeography of *Padina boryana* (Dictyotales, Phaeophyceae) around the Thai-Malay Peninsula. Ph.D. dissertation Prince of Songkhla University, Hat Yai, Thailand. 2014;57 pp.
29. Deb B, Uddin A, Chakraborty S. Composition, codon usage pattern, protein properties, and influencing factors in the genomes of members of the family Anelloviridae. *Arch Virol.* 2021;166(2):461–74.
30. Kim H, Yang JH, Bustamante DE, Calderon MS, Mansilla A, Maggs CA, et al. Organelle genome variation in the red algal genus *Ahnfeltia* (Florideophyceae). *Front Genet.* 2021;12:724–34.
31. Lee JM, Song HJ, Park SI, Lee YM, Jeong SY, Cho TO, et al. Mitochondrial and plastid genomes from coralline red algae provide insights into the incongruent evolutionary histories of organelles. *Genome Biol Evol.* 2018;10(11):2961–72.
32. Smith DR. Mutation rates in plastid genomes: they are lower than you might think. *Genome Biol Evol.* 2015;7(5):1227–34.
33. Smith DR, Keeling PJ. Mitochondrial and plastid genome architecture: reoccurring themes, but significant differences at the extremes. *Proc Natl Acad Sci U S A.* 2015;112(33):10177–84.
34. Choi JW, Graf L, Peters AF, Cock JM, Nishitsuji K, Arimoto A, et al. Organelle inheritance and genome architecture variation in isogamous brown algae. *Sci Rep.* 2020;10(1):2048.
35. Maier UG, Fraunholz M, Zauner S, Penny S, Douglas S. A nucleomorph-encoded CbbX and the phylogeny of RuBisCo regulators. *Mol Biol Evol.* 2000;17(4):576–83.
36. Mohanta TK, Khan A, Khan AL, Hashem A, Abd Allah EF, Al-Harassi A. Gene loss and evolution of the plastome. *Genes.* 2020;11(10):1133.
37. Han KY, Maciszewski K, Graf L, Yang JH, Andersen RA, Karnkowska A, et al. Dictyochophyceae plastid genomes reveal unusual variability in their organization. *J Phycol.* 2019;55(5):1166–80.
38. Kim Ji, Shin H, Škaloud P, Jung J, Yoon HS, Archibald JM, et al. Comparative plastid genomes of Synurophyceae: inverted repeat dynamics and gene content variation. *BMC Evol Biol.* 2019;19(1):20–33.
39. Maréchal A, Brisson N. Recombination and the maintenance of plant organelle genome stability. *New Phytol.* 2010;186(2):299–317.
40. Goulding SE, Olmstead RG, Morden CW, Wolfe KH. Ebb and flow of the chloroplast inverted repeat. *Mol Gen Genet.* 1996;252(1–2):195–206.
41. Cattolico RA, Jacobs MA, Zhou Y, Chang J, Duplessis M, Lybrand T, et al. Chloroplast genome sequencing analysis of *Heterosigma akashiwo* CCMP452 (West Atlantic) and NIES293 (West Pacific) strains. *BMC Genomics.* 2008;9:211.
42. Lommer M, Roy AS, Schilhabel M, Schreiber S, Rosenstiel P, LaRoche J. Recent transfer of an iron-regulated gene from the plastid to the nuclear genome in an oceanic diatom adapted to chronic iron limitation. *BMC Genomics.* 2010;11:718.
43. Su Y, Huang L, Wang Z, Wang T. Comparative chloroplast genomics between the invasive weed *Mikania micrantha* and its indigenous congener *Mikania cordata*: Structure variation, identification of highly divergent regions, divergence time estimation, and phylogenetic analysis. *Mol Phylogenet Evol.* 2018;126:181–95.
44. Palmer JD. Chloroplast DNA exists in two orientations. *Nature.* 1983;301:92–3.
45. Hansen DR, Dastidar SG, Cai Z, Penafior C, Kuehl JV, Boore JL, et al. Phylogenetic and evolutionary implications of complete chloroplast genome sequences of four early-diverging angiosperms: *Buxus* (Buxaceae), *Chloranthus* (Chloranthaceae), *Dioscorea* (Dioscoreaceae), and *Illicium* (Schisandraceae). *Mol Phylogenet Evol.* 2007;45:547–63.
46. Fullerton SM, Bernardo Carvalho A, Clark AG. Local rates of recombination are positively correlated with GC content in the human genome. *Mol Biol Evol.* 2001;18(6):1139–42.
47. Walker JF, Zanis MJ, Emery NC. Comparative analysis of complete chloroplast genome sequence and inversion variation in *Lasthenia burkei* (Madieae, Asteraceae). *Am J Bot.* 2014;101:722–9.
48. Smith NG, Webster MT, Ellegren H. Deterministic mutation rate variation in the human genome. *Genome Res.* 2002;12(9):1350–6.
49. Bi YH, Feng B, Xie WY, Ouyang LL, Ye RX, Zhou ZG. Nuclear-encoded CbbX located in chloroplast is essential for the activity of red-type Rubisco in *Saccharina japonica*. *Plant Physiol Biochem.* 2023;196:236–45.
50. Smith DR, Arrigo KR, Alderkamp AC, Allen AE. Massive difference in synonymous substitution rates among mitochondrial, plastid, and nuclear genes of *Phaeocystis* algae. *Mol Phylogenet Evol.* 2014;71:36–40.
51. Smith DR, Hua J, Lee RW, Keeling PJ. Relative rates of evolution among the three genetic compartments of the red alga *Porphyra* differ from those of green plants and do not correlate with genome architecture. *Mol Phylogenet Evol.* 2012;65:339–44.

52. Drouin G, Daoud H, Xia J. Relative rates of synonymous substitutions in the mitochondrial, chloroplast and nuclear genomes of seed plants. *Mol Phylogenet Evol.* 2008;49:827–31.
53. Wang H, Meng T, Wei W. Analysis of synonymous codon usage bias in helicase gene from *Autographa californica* multiple nucleopolyhedrovirus. *Genes Genom.* 2018;40(7):767–80.
54. Bolger AM, Lohse M, Usadel B. Trimmomatic: a flexible trimmer for Illumina sequence data. *Bioinformatics.* 2014;30:2114–20.
55. Altschul SF, Gish W, Miller W, Myers EW, Lipman DJ. Basic local alignment search tool. *J Mol Biol.* 1990;215(3):403–10.
56. Katoh K, Standley DM. MAFFT multiple sequence alignment software version 7: improvements in performance and usability. *Mol Biol Evol.* 2013;30(4):772–80.
57. Talavera G, Castresana J. Improvement of phylogenies after removing divergent and ambiguously aligned blocks from protein sequence alignments. *Syst Biol.* 2007;56(4):564–77.
58. Nguyen LT, Schmidt HA, von Haeseler A, Minh BQ. IQ-TREE: a fast and effective stochastic algorithm for estimating maximum-likelihood phylogenies. *Mol Biol Evol.* 2015;32:268–74.
59. Guindon S, Dufayard JF, Lefort V, Anisimova M, Hordijk W, Gascuel O. New algorithms and methods to estimate maximum-likelihood phylogenies: assessing the performance of PhyML 3.0. *Syst Biol.* 2010;59:307–21.
60. Minh BQ, Nguyen MA, von Haeseler A. Ultrafast approximation for phylogenetic bootstrap. *Mol Biol Evol.* 2013;30:1188–95.
61. Ronquist F, Teslenko M, van der Mark P, Ayres DL, Darling A, Höhna S, et al. MrBayes 3.2: efficient Bayesian phylogenetic inference and model choice across a large model space. *Syst Biol.* 2012;61(3):539–542.
62. Kalyaanamoorthy S, Minh BQ, Wong TKF, von Haeseler A, Jermini LS. ModelFinder: fast model selection for accurate phylogenetic estimates. *Nat Methods.* 2017;14(6):587–9.
63. Chen CJ, Chen H, Zhang Y, Thomas HR, Frank MH, He Y, et al. TBtools: An integrative toolkit developed for interactive analyses of big biological data. *Mol Plant.* 2020;13(8):1194–202.
64. Darling AC, Mau B, Blattner FR, Perna NT. Mauve: multiple alignment of conserved genomic sequence with rearrangements. *Genome Res.* 2004;14(7):1394–403.
65. Li H, Guo Q, Xu L, Gao H, Liu L, Zhou X. CPJSDraw: analysis and visualization of junction sites of chloroplast genomes. *PeerJ.* 2023;11:e15326.
66. Lowe TM, Chan pp. tRNAscan-SE on-line: Search and contextual analysis of transfer RNA genes. *Nucl Acids Res.* 2016;44:W54–57.
67. Zhang D, Gao F, Jakovlić I, Zou H, Zhang J, Li WX, et al. PhyloSuite: An integrated and scalable desktop platform for streamlined molecular sequence data management and evolutionary phylogenetics studies. *Mol Ecol Resour.* 2020;20(1):348–55.
68. Yang Z. PAML 4: a program package for phylogenetic analysis by maximum likelihood. *Mol Biol Evol.* 2007;24(8):1586–91.
69. Beier S, Thiel T, Münch T, Scholz U, Mascher M. MISA-web: a web server for microsatellite prediction. *Bioinformatics.* 2017;33(16):2583–5.
70. Kurtz S, Schleiermacher C. Reputer: fast computation of maximal repeats in complete genomes. *Bioinformatics.* 1999;15(5):426–7.
71. Peden, John F. Analysis of codon usage. Univ. Nottingham. 2000;90(1):73–74.
72. Behura SK, Severson DW. Comparative analysis of codon usage bias and codon context patterns between dipteran and hymenopteran sequenced genomes. *PLoS ONE.* 2012;7(8):e43111.

Publisher's Note

Springer Nature remains neutral with regard to jurisdictional claims in published maps and institutional affiliations.